Scientific African 15 (2022) e01129

Contents lists available at ScienceDirect

Scientific African

journal homepage: www.elsevier.com/locate/sciaf

Landslide hazard zonation and evaluation around Debre Markos town, NW Ethiopia—a GIS-based bivariate statistical approach

Dawit Asmare

Engineering Geology, DMiT, Debre Markos University, PO Box 269, Debre Markos, Ethiopia

ARTICLE INFO

Article history:
Received 10 September 2021
Revised 31 January 2022
Accepted 16 February 2022

Edited DR B Gyampoh

Keywords:
Geographical information system
Bivariate statistical
Landslide hazard zonation
Landslide hazard evaluation
Hazard index
Landslide inventory

ABSTRACT

The main purpose of this study was to perform landslide hazard zonation and evaluation around Debre Markos town, Northwest Ethiopia. This was achieved using a GIS-based bivariate statistical technique. Initially, a landslide inventory map containing information on past and active landslide locations was prepared. In this study, eight conditioning factors, including slope material (lithology and soil mass), elevation, aspect, slope, land use, land cover, curvature, distance to fault, and distance to drainage, were identified and integrated with the ArcGIS platform. Data were collected from field mapping, satellite images, and digital elevation models. All conditioning factors were statistically analyzed to determine their relationship to previous landslides. The hazard map revealed that 17.15% (40.60 km2) of the study area falls under no hazard zone, 25.53% (60.45 km2) in low hazard zone, 28.04% (66.39 km2) in moderate hazard zone, 18.93% (44.83 km2) in high hazard zone, and the remaining 10.36% (24.54 km2) in very high hazard zone. The validation of the landslide hazard zonation map shows that 94% of past landslides fall in high or very high hazard zones, while 3% fall in moderate hazard zone, 2% fall in low hazard zone, and 1% fall in no hazard zone. The validation of the LHZ map thus, reasonably showed that the adopted methodology produced satisfactory results. The delineated hazard zones may practically be applied for the regional planning and development of infrastructures in the area. The results also indicated that slope angle, distance to fault, distance to drainage, and slope material types were statistically significant in controlling the landslides.

© 2022 The Author(s). Published by Elsevier B.V. on behalf of African Institute of Mathematical Sciences / Next Einstein Initiative.
This is an open access article under the CC BY-NC-ND license (http://creativecommons.org/licenses/by-nc-nd/4.0/)

Introduction

Landslides are the most frequent and severe geologic hazards in hilly areas, causing immediate economic harm, property damage and repair costs, injuries, and death [1–11,16,73]. The Ethiopian highlands are defined by variable topographical, geological, soil cover, hydrological (surface and groundwater), and land-use conditions [5,12–18]. These highlands are frequently affected by rainfall-triggered slope failures [5].

Landslides are caused by a variety of geo-environmental processes, including geological, metrological, and human activities [1,19–23]. According to Raghuvanshi et al [14]., slope geometry, slope material, structural discontinuities, land use land

E-mail address: dawitasmare55@gmail.com

https://doi.org/10.1016/j.sciaf.2022.e01129
2468-2276/© 2022 The Author(s). Published by Elsevier B.V. on behalf of African Institute of Mathematical Sciences / Next Einstein Initiative. This is an open access article under the CC BY-NC-ND license (http://creativecommons.org/licenses/by-nc-nd/4.0/)

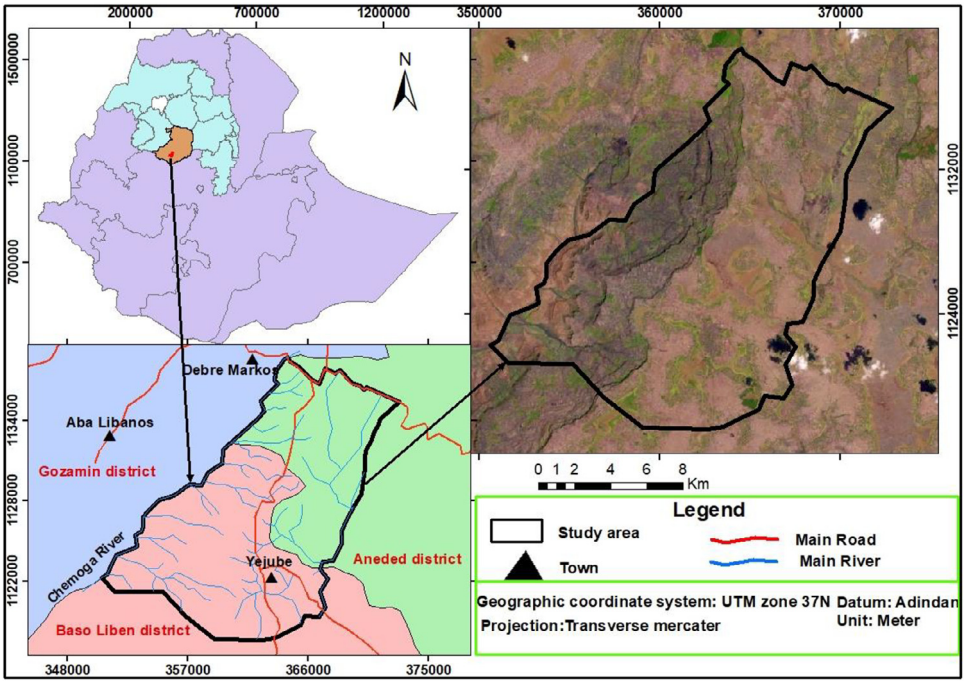

Fig. 1. Study area.

cover, slope geometry, and groundwater are the main internal conditioning factors, while excessive rainfall, earthquakes, and man-made activities can be considered as the main conditioning factors for landslides.

Landslide hazard zonation was carried out using various approaches that have been suggested by early researchers to improve the prediction accuracy of landslides. The statistically based methods assess the correlation between the landslide conditioning factors and the landslide occurrence [23–28]. Such approaches have been used to produce landslide susceptibility maps assisted by geographic information system (GIS) technology. Generally, the existing approaches can be grouped into three main classes: deterministic, statistical, and expert evaluation approaches [14,29–34]. Bivariate and multivariate statistical models, such as frequency ratio [7,35–39], weights-of-evidence [21,28,40–45], logistic regression [6,24,25,27,31,46–49] models, have been widely used by early researchers. Expert knowledge-based models, such as the analytical hierarchy process (AHP) model [1,7,24,50–52] and fuzzy approaches [21,53–55], are common in different literature. Selection of approaches for landslide hazard zoning depends on the size of the analysis to be performed, the total coverage area, expertise, and skill set of evaluators, and the geological or geomorphic parameters or methods used to produce parameter data [1,19,23,27,56].

Thus, for the current study, a bivariate statistical approach was followed. In the bivariate statistical approach, each factor is compared to a landslide inventory map. This approach is considered to be simple, applicable, robust, and flexible. However, it has several limitations, including loss of data quality and accuracy with the oversimplification of input thematic data and loss of data sensitivity in forced individual analysis of conditioning factors [57,58].

The present study area is characterized by extremely rugged topography and high altitude ranges. Several landslides have occurred in the last few years in this area. People have been permanently displaced from their residences as they have lost their houses and farm plots. However, no published or unpublished study on landslides has been reported from the area prior to the present study. Therefore, this area requires a detailed investigation to reduce the damage to infrastructures, houses, cultivated lands, and loss of lives. The main objective of this study was to produce a landslide hazard zonation (LHZ) map for the area. For LHZ map preparation, a GIS-based bivariate statistical approach was followed.

Study area

The study area is located in the Amhara Regional State of Ethiopia, Northwestern Ethiopian Plateau (NWEP). The study area includes parts of the Aneded and Baso Liben districts (Fig. 1). It covers a total area of 236.8 km2 and the altitudes range from 1283 to 2500 m. The mean annual rainfall in the study area lies within the high class (i.e., 1101–1500 mm). The mean annual precipitation is around 700 mm, most of which precipitation occurs from June to the end of September. The maximum mean annual precipitation in the present study area is high, and the highest monthly precipitation was recorded in July. The study area mainly consists of various lithological formations such as basalt, sandstone, alluvial deposits, colluvial deposits, and residual soils.

Table 1
Conditioning factors and their respective data sources.

No.	Conditioning factors	GIS data type	Scale	Data Source
1	Landslide inventory	Polygon	1:50,000	Field observation GPS point data, Google Earth image (2021)
2	Slope material	Polygon	1:50,000	Geological map of Ethiopia (Tefera et al., 1996), Field observations
3	Elevation	Grid	30 × 30	DEM Data (30 × 30 m) ASTER data set
4	Aspect	Grid	30 × 30	
5	Slope	Grid	30 × 30	
6	Curvature	Grid	30 × 30	
7	Land use land cover	Grid	30 × 30	Google Earth image (2021), Landsat image, Field observations
8	Distance to fault	Grid	1:50,000	Topographical map (1:50,000), Google Earth image (2021), Field observation GPS point data
9	Distance to drainage	Grid	30 × 30	DEM Data (30 × 30 m) ASTER data set

Data preparation

All pertinent data required for landslide hazard evaluation were collected from primary and secondary data sources. Secondary data include topographical maps, geological maps, satellite images, and digital elevation models (DEM 30 m) (Table 1). Primary data were collected in the field. A field investigation was mainly undertaken to obtain all the relevant information about the past landslide activities in the area and to verify various conditioning factor maps prepared during the pre-field works. During the field investigations, a geological map from the literature was checked, the lithologic units were identified, and the landslide inventory map was prepared.

Landslide inventory

A landslide inventory map is important for landslide hazard mapping. It is widely accepted that the conditions that caused previous landslides can cause landslides again if they occur elsewhere in a given area [6,23,27,59,60].

A landslide inventory map was prepared using landslide locations identified from satellite images, field checks, and Google Earth image interpretation. A detailed field investigation was conducted to determine the spatial locations and nature of landslides for the preparation of an inventory. The landslide inventory map of the study area was created by overlaying field GPS failure point data on the DEM_30 m by using Arc GIS (Fig. 3I). All the maps in this study were produced at a scale of 1:50,000. During field work, most past landslides were observed along with fault segments. Besides, there are also a significant number of landslides along the river valleys (Fig. 2).

Landslide conditioning factors

For the present study, eight prominent conditioning factors were considered for landslide hazard zonation mapping. These include slope material (lithology and soil mass), elevation, aspect, slope, land use land cover, curvature, distance to fault, and distance to drainage. Generally, these possible landslide conditioning factors were selected based on the nature of the study area and the availability and suitability of data. The various data sources were used to prepare spatial data sets for these conditioning factors (Table 1).

In this study, a DEM_30 m was used to produce elevation, aspect, slope angle, land use land cover, curvature, distance to fault, and distance to drainage maps.

Lithology and soil mass

The lithology has a significant effect on slope stability; various lithological units have varying degrees of susceptibility [37]. Lithology has a significant impact on the stability of the soil, natural ground cover, and features created by human activities [61]. Landslides are more likely in areas where the rocks are weak, poorly consolidated, and incompetent [62].

The lithological map of the research area was updated from the geological map produced by Tefera et al. (1996) (Fig. 3A). Past landslide distribution among various lithologies shows that 10.5% of the landslides occurred in the Adigrat formation, 1.8% within the Ashangi formation, and 1.6% were recorded in the Tarmaber formation. In the case of soil mass, 51.5% of the landslides occurred in the colluvial deposit, 23.7% within the alluvial deposit, and 10.9% of the landslides occurred in the residual soil.

Ground surface slope

Slope angle is among the most important factors influencing landslides [61,62] because it is directly linked to landslides [58]. In general, the steeper the slope, the greater the likelihood of a landslide [62]. Gravity pulls are directly related to the slope angle, which is the primary driving force for slope failure [23,63]. In this study, the slope angle map was classified

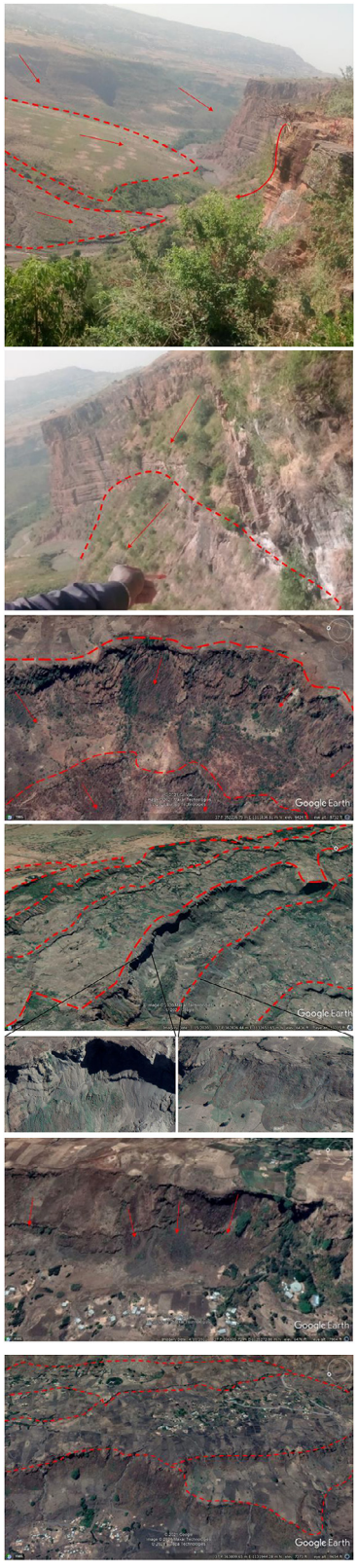

Fig. 2. Samples of landslides in the study area.

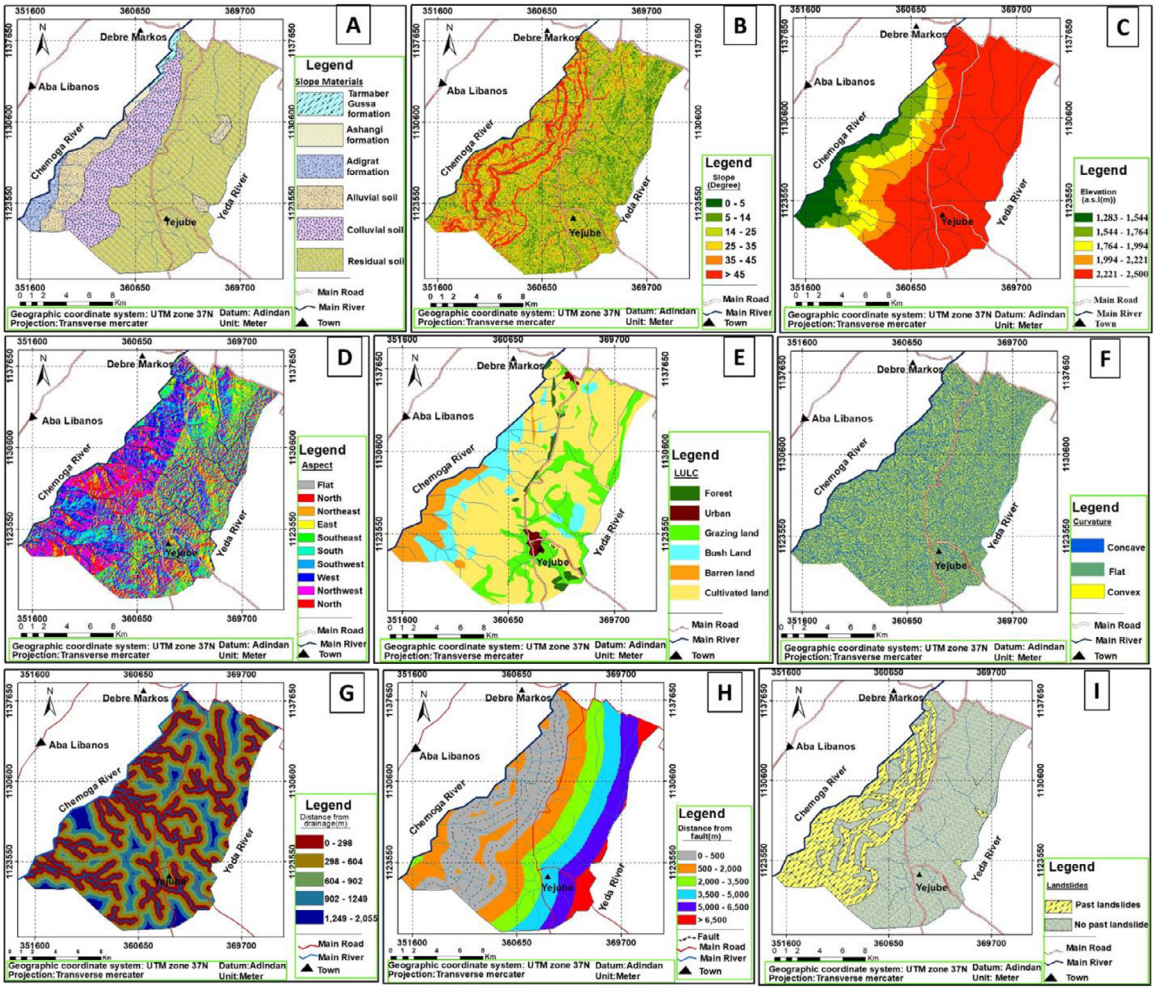

Fig. 3. Lithology and Soil Mass(A), Slope(B), Elevation(C), Aspect(D), LULC(E), Curvature(F), Distance to Drainage(G), Distance to Fault(H), Landslide Inventory (I).

into five classes; very gentle slope (<15°), gentle slope (16–25°), moderately steep slope (26–35°), steep slope (36–45°), and escarpment /cliff (>45°) (Fig. 3B).

According to the landslide inventory data, the spatial and potential distribution of landslides reveals that 1.6%, 11.3%, 22.4%, 21%, 16.7%, and 27% of the landslides occurred in the slope classes between 0 and 5°, 5–14°, 14–25°, 25–35°, 35–45°, and 45°, respectively.

Elevation

Higher elevation areas have a higher possibility of landslide occurrence than lower elevation areas [31,40,62,64].

In this study, the elevation map was classified into five classes: 1283–1544 m, 1544–1764 m, 1764–1994 m, 1994–2221 m, and 2221–2500 m (Fig. 3C). Past landslide distribution among various elevation classes shows that 18.5%, 21.1%, 17.8%, 23%, and 18.9% of the landslides occurred in the elevation classes from 1283 to 1544 m, 1544–1764 m, 1764–1994 m, 1994–2221 m, and 2221–2500 m, respectively.

Aspect

The direction of the slope with respect to the sunlight has a huge effect on the structural and chemical composition of the slope [22,37,65]. In this study, the aspect map was classified into nine classes; Flat (−1°), North (0–22.5°), Northeast (22.5–67.5°), East (67.5–112.5°), Southeast (112.5–157.5°), South (157.5–202.5°), Southwest (202.5–247.5°), West (247.5–292.5°), Northwest (292.5–337.5°), and North (337.5–360) (Fig. 3D).

The distribution of past landslides in the area with respect to aspect reveals that 27.1% of the landslides occurred in slopes facing toward the Northwest, 24.1% in the West, 15.9% in the North, 13.7% in the Southwest, 6.5% in the South, and

6.1% in the Northwest directions. The remaining landslides occurred in slopes facing Southeast (3.6%), East (3%), and flat (0.02%) directions.

Land use land cover

The strength of slope materials against sliding and the regulation of slope water content are affected by land use land cover [24,66]. Furthermore, plant roots strengthen the slope and are commonly regarded as reinforcements [67,68]. Land cover absorbs soil water and decreases the probability of a landslide [24,69].

A Google Earth image and Landsat images data source were used to develop a land use land cover map. Then, the map was modified and updated based on visual field observations, and the final map was produced (Fig. 3E) in Arc GIS.

The distribution of landslides within various land use and land cover classes shows that 51% of landslides occurred within cultivated land. Barren land, bushland, forest cover, and grazing land account for 24.2%, 22.6%, 1.4%, and 0.8%, respectively.

Curvature

The morphology of the topography is represented by the curvature values [70]. This factor affects landslide occurrence while controlling surface runoff [71]. In this study, the curvature map was classified into three main classes: negative curvature (concave (<0)), zero curvature (flat (0)), and positive curvature (convex (>0)) (Fig. 3F). The slope's concavity is shown by a negative curvature value, while the slope's convexity is shown by a positive curvature value. High convexity and concavity cause drainage concentration across space, resulting in slope saturation and instability [38]. Past landslide distribution shows that 49.2% of landslides occurred in concave slope (<0), 1.2% in flat slope (0), and 49.6% in convex slope (>0).

Distance to drainage

The saturation degree of the slope's material is a significant parameter that governs its stability [37,58]. Distance to drainage is one of the most important parameters in landslide studies [58]. River water is considered the main source of soil moisture [71]. Distance to drainage lines of intensive gully erosion is a crucial factor in controlling the occurrence of landslides [70].

In this study, the distance to drainage was generated by Euclidean distance in Arc GIS, then reclassified into five classes: 0–298 m, 298–604 m, 604–902 m, 902–1249 m, and 1249–2055 m (Fig. 3G). The distribution of landslides from previous landslide inventory data revealed that 44.9%, 25.5%, 15.5%, 9.5%, and 4.5% of the landslides occurred in the drainage distance classes of 0–298 m, 298–604 m, 604–902 m, 902–1249 m, and 1249–2055 m, respectively.

Distance to fault

Geological structures, including folds, joints, bedding, and shear zone faults, have a significant impact on slope stability [72]. The proximity of a slope to these features has a significant impact on its stability, increasing the probability of landslides occurring [72]. The number of joints in a rock reduces its strength, which increases the distance to faults and lineaments.

The fault map was created using a topographical map (1:50,000), Google Earth image, field observation, and DEM_30 m. The distance to the fault was generated by Euclidean distance in Arc GIS, then reclassified into six classes: 0–500 m, 500–2000 m, 2000–2500 m, 2500–5000 m, 5000–6500 m, and > 6500 m (Figure 3H). The distribution of landslides from past landslide inventory data revealed that 77.9%, 20%, 0.9%, 0.1%, 1%, and 0.1% of the landslides occurred in the fault distance class between 0 and 500 m, 500–2000 m, 2000–2500 m, 2500–5000 m, 5000–6500 m, and greater than 6500 m, respectively.

Methodology

In this research, a bivariate statistical system was applied to develop an LHZ map. In this system, the main objective is to derive the densities of landslide occurrences within each conditioning factor map and its parameter map classes. Later, based on the class distribution and the landslide density, respective weights can be derived. This system can provide practical interactions between different conditioning factors and the past and present distribution of landslides [12,13,73]. For statistical methods, it is believed that landslides may occur again if the conditions that caused previous landslides reoccur in other areas in the future [12,13,23].

To rate the various conditioning factors likely to be responsible for the reoccurrence of landslides with similar conditions in the area, a quantitative prediction was developed based on the density ratio of the past landslides with respect to respective factor classes [12,13,74]. Later, with the derived ratings for various conditioning factors, each of the factor maps was analyzed and combined in a GIS environment to produce an LHZ map. For the present study, eight conditioning factors, namely, slope material (lithology and soil mass), elevation, aspect, slope, land use land cover, curvature, distance to fault, and distance to drainage, were considered. These are the significant conditioning factors possibly responsible for past landslides in the area. All these factors were individually evaluated in a GIS environment to know the respective densities of the

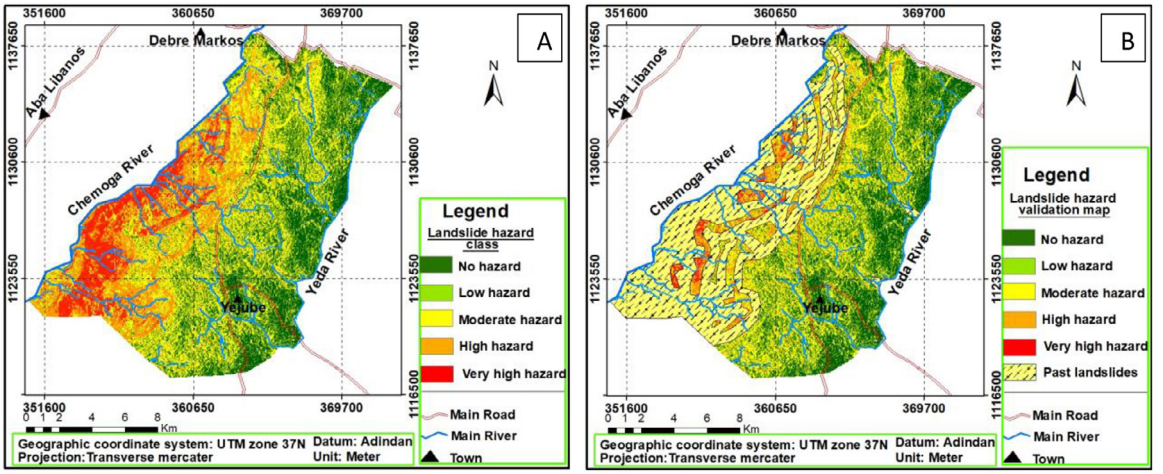

Fig. 4. (A) Landslide Hazard Zonation, (B) Overlaid Validation map7. Conclusion.

past landslides within each of the factor classes. These are the significant conditioning factors possibly responsible for past landslides in the area. All these factors were individually evaluated in a GIS environment to know the respective densities of the past landslides within each of the factor classes. Using the tool raster calculator in Arc GIS, the total pixels occupied by each factor class and the total pixels covered by the landslides within the respective factor classes were assessed. The hazard index value for each conditioning factor is the ratio between landslides that "did occur" and landslides that "did not occur" derived for every factor subclass [12,13] (Tables 1 and 2). In the present study area, the total pixel count for the whole study area was 263,112, of which 80,276 pixels were covered by active landslides. Later, as per these hazard index values, appropriate weight was assigned to each of the conditioning factors ([37,75–78]). Further, based on these hazard index values and by assigning suitable weights to each factor, random trial combinations were attempted to produce the LHZ map [12–13,38]. Finally, the prepared LHZ map was validated with the past landslides in the area (Fig. 4B).

Landslide hazard zonation (LHZ)

In this research, slope material (lithology and soil mass), slope, aspect, elevation, curvature, land use land cover, distance from drainage, and distance from the fault were identified as conditioning factors. It was believed that these conditioning factors were most likely to account for the landslides in the area.

The hazard map for each of the eight conditioning factors was prepared using a weight equal to 1 (Table 3). The possible explanation for assigning equal weight to all different internal and external conditioning factors is that the relative contribution of each parameter to slope failure cannot be quantified. Therefore, it was assumed that each of these factors would have a relative contribution to slope failure. Using the "raster calculator" tool and ratings, a landslide hazard zonation map of the area was produced as shown in Fig. 4A. The classification of Hazard (x) values presented in Table 4 provided the most reliable validation results with the past landslide data in the present study area.

Results and discussion

In this study, after preparing a landslide inventory map, eight conditioning factors have been considered. The main conditioning factor for all past landslides in the study area, as reported, was rainfall, as all past landslides occurred during the rainy season. As mentioned earlier, the maximum mean annual precipitation in the present study area is high, and the highest monthly precipitation was recorded in July. This rainfall-induced landslide in the study area possibly occurred as a result of shear strength reduction of the slope material due to saturation and development of pore water pressures within the slope mass [23]. This is evident because the majority of previous landslides in the study area occurred on slopes composed of colluvial and alluvial soils.

Elevation has an important influence on the occurrence of landslides [23]. In general, most of the past landslides (23%) occurred in the elevation class of 1994–2221 m, whereas 21.1% of the landslides have occurred in the elevation class of 1544–1764 m. The dominance of landslides in these elevation ranges may be due to existing fault escarpments and poor agricultural practices. Besides, the slope angle is an important factor in controlling the stability of the slope [23]. It was found that the majority of the past landslides in the study area have occurred on steep slopes or fault escarpments ($> 45°$). Generally, as the slope increases, the probability of landslide occurrence also increases.

Cultivated land showed a high frequency (51%) of past landslides. Similarly, this may be related to poor irrigation practice, which might have resulted in the instability of slopes. Also, the cultivation land in the study area mostly comprises colluvial or alluvial soils, which are prone to instability. Poor irrigation and frequent plowing practices make such colluvial material

Table 2
Hazard index for various classes of conditioning factors.

conditioning factors and corresponding factor class	landslide did not occur		landslide occurs		Hazard index (b/a)	Percent landslide
	Count	Ratio (a) (%)	Count	Ratio (b) (%)		
(a) Lithology						
Adigrat formation	150	0.08	8418	10.49	127.26	86.06
Ashangi formation	429	0.23	1443	1.8	7.67	5.19
Tarmaber formation	1719	0.94	1297	1.61	1.72	1.16
Alluvial soil	6716	3.67	18,991	23.66	6.44	4.35
Colluvial soil	20,217	11.06	41,349	51.51	4.66	3.15
Residual soil	153,605	84.01	8778	10.94	0.13	0.09
Total	182,836	100	80,276	100	147.87	100
(b) Slope(degree)						
0–5	22,197	12.14	1310	1.63	0.13	1.61
5–14	13,450	7.36	9110	11.35	1.54	18.44
14–25	17,956	9.82	17,981	22.40	2.28	27.27
25–35	69,471	38	16,859	21	0.55	6.61
35–45	44,192	24.17	13,393	16.68	0.69	8.25
>45	15,570	8.52	21,623	26.94	3.16	37.82
Total	182,836	100	80,276	100	8.36	100
(c) Aspect						
Flat	117	0.06	14	0.02	0.27	2.87
N	11,508	6.29	5203	6.48	1.03	10.83
Ne	21,390	11.7	4929	6.14	0.52	5.52
E	22,599	12.36	2419	3.01	0.24	2.56
Se	23,520	12.86	2887	3.6	0.28	2.94
S	21,956	12.01	5207	6.49	0.54	5.68
Sw	23,173	12.67	11,026	13.74	1.08	11.4
W	23,719	12.97	19,313	24.06	1.85	19.51
Nw	24,457	13.38	21,716	27.05	2.02	21.27
Nnw	10,397	5.69	7562	9.42	1.66	17.42
Total	182,836	100	80,276	100	9.51	100
(d) Elevation (m)						
1283–1544	1078	0.59	14,998	18.68	31.68	65.29
1544–1764	5302	2.9	16,944	21.11	7.28	15
1764–1994	7394	4.04	14,266	17.77	4.39	9.06
1994–2221	8781	4.8	19,112	23.81	4.96	10.22
2221–2500	160,280	87.66	14,956	18.63	0.21	0.44
Total	182,836	100	80,276	100	48.52	100
(e) Landuse/ landcover						
Forest	3296	1.8	1122.5	1.40	0.78	1.43
Urban	3222	1.76	0	0	0	0
Grazing land	40,909	22.37	634.5	0.79	0.04	0.07
Bush land	11,113	6.08	18,159.8	22.62	3.72	6.86
Barren land	904	0.49	19,427.5	24.2	48.93	90.25
Cultivated land	123,391	67.49	40,931.8	50.99	0.76	1.39
Total	182,836	100	80,276	100	54.22	100
(F) Curvature						
Concave (+ve)	89,883	49.16	39,551	49.27	1	36.49
Flat (0)	2705	1.48	877	1.09	0.74	26.89
Convex (-ve)	90,248	49.36	39,848	49.64	1.01	36.62
Total	182,836	100	80,276	100	2.75	100
(G) Distance from fault						
0–500	24,449	13.37	62,576.5	77.95	5.83	85.74
500–2000	42,633	23.32	16,070.5	20.02	0.86	12.63
2000–2500	38,107	20.84	765.5	0.95	0.05	0.67
2500–5000	36,219	19.81	67.5	0.08	0	0.06
5000–6500	31,689	17.33	773.5	0.96	0.06	0.82
> 6500	9738	5.33	22.5	0.03	0.01	0.08
Total	182,836	100	80,276	100	6.8	100
(H) Distance from drainage						
0–298	58,468	31.98	36,003.4	44.85	1.4	28.6
298–604	52,082	28.49	20,484.4	25.52	0.9	18.27
604–902	39,240	21.46	12,524.4	15.6	0.73	14.82
902–1249	26,208	14.33	7608.4	9.48	0.66	13.48
1249–2055	6840	3.74	3655.4	4.55	1.22	24.82
Total	182,836	100	80,276	100	4.9	100

Table 3
Weightings, hazard index, and hazard class for conditioning factors.

conditioning factors (j)	conditioning factors class (i)	Weighting (Wj)	Hazard index (Hji)	Hazard index scaled to 1 (Hji)	Hazard class
Lithology	Adigrat formation	1	127.26	1	5
	Ashangi formation		7.67	0.06	2
	Tarmaber formation		1.72	0.01	1
	Alluvial soil		6.44	0.05	1
	Colluvial soil		4.66	0.04	1
	Residual soil		0.13	0	1
Slope (degree)	0–5	1	0.13	0.04	1
	5–14		1.54	0.49	4
	14–25		2.28	0.72	4
	25–35		0.55	0.17	3
	35–45		0.69	0.22	4
	>45		3.16	1	5
Aspect	Flat	1	0.27	0.13	3
	N		1.03	0.51	4
	NE		0.52	0.26	4
	E		0.24	0.12	2
	SE		0.28	0.14	3
	S		0.54	0.27	4
	SW		1.08	0.54	4
	W		1.85	0.92	5
	NW		2.02	1	5
	NNW		1.66	0.82	5
Elevation (m)	1283–1544	1	31.68	1	5
	1544–1764		7.28	0.23	4
	1764–1994		4.39	0.14	3
	1994–2221		4.96	0.16	3
	2221–2500		0.21	0.01	1
Land use/landcover	forest	1	0.78	0.02	1
	urban		0	0	1
	grazing land		0.04	0	1
	bushland		3.72	0.08	2
	barren land		48.93	1	5
	cultivated land		0.76	0.02	1
Curvature	concave (+ve)	1	1	0.99	5
	flat (0)		0.74	0.73	4
	convex (-ve)		1.01	1	5
Distance from fault	0–500	1	5.83	1	5
	500–2000		0.86	0.15	3
	2000–2500		0.05	0.01	1
	2500–5000		0	0	1
	5000–6500		0.06	0.01	1
	> 6500		0.01	0	1
Distance from drainage	0–298	1	1.40	1.00	5
	298–604		0.90	0.64	4
	604–902		0.73	0.52	4
	902–1249		0.66	0.47	4
	1249–2055		1.22	0.87	5

loose and saturated, which reduces the shear strength considerably [23]. Thus, such material may result in instability of the slope.

In the present study, 51.5% of past landslides have occurred in colluvial soil slopes, whereas about 23.7% of landslides were observed in alluvial soils. Not many landslides were recorded from slopes formed by rocks. It is reasonable to understand that colluvial soils are loose soils that may be comprised of angular to sub-angular rock fragments of variable dimensions in a matrix of sandy silty soils. Such material possesses low shear strength and, when saturated, may result in the washing of finer particles and may become more prone to instability [14].

Past landslide data indicates that 77.9% of past landslides occurred within slopes, which are at a distance < 500 m from fault escarpments. This showed that slopes close to fault escarpments may have a higher probability of instability. In the case of the relationship between landslide occurrence and the distance from drainage, as the distance from drainage increases, the occurrence of landslides generally decreases. Similarly, 44.9% of past landslides occurred within slopes, which are at a distance < 298 m. This showed that most of the past landslides were initiated by the nearest drainage valley in the study area. The saturation degree of the materials on the slope and closeness of the slope to drainage structures is an important parameter for the control of slope stability [7,79].

Table 4
Hazard index classification [76].

Hazard class	Hazard index (Hji) classification	Hazard class name
1	0.0–0.05	No hazard (NH)
2	0.05–0.12	Low hazard (LH)
3	0.12–0.18	Medium hazard (MH)
4	0.18–0.75	High hazard (HH)
5	0.75–1.0	Very high hazard (VHH)

Further, it was observed that the concentration of past landslides is in slopes facing northwest, west, and southwest directions. Aspect is related to parameters such as exposure to sunlight, winds (dry or wet), rainfall (degree of saturation), soil moisture, and discontinuities that may control the occurrence of landslides [7,73]. The northwest, west, and southwest aspects of the study area, which is receiving excessive sun radiation and high rainfall, are more prone to landslides. In the case of curvature, the majority of the present study area showed concave slopes (>0) and convex slopes (<0) curvature classes. The more positive or negative values indicate a higher probability of landslide occurrence [7].

The resulting landslide hazard map (Fig. 4A) shows that 17.15% (40.60 km2), 25.53% (60.45 km2), 28.04% (66.39 km2), 18.93% (44.83 km2), and 10.36% (24.54 km2) of area fall into the no hazard, low, moderate, high, and very high hazard classes, respectively. Consequently, a glance at Fig. 4A reveals that very high hazard (VHH) areas generally fall in the southwestern parts of the areas, while the southern and southwestern parts are demarcated as high hazard (HH) zones, with a scarce distribution in the eastern and northern parts. In addition, moderate hazard (MH) zones are widely distributed in the eastern and northern regions, while low hazard (LH) zones are distributed in the northwestern region of the research area. More dispersed low-hazard areas are also found in the central and eastern regions. No hazard (NH) areas are mostly clustered in the north, with a sparse distribution in the west and east.

The prevalence of colluvial and alluvial soils, relatively gentle slopes (14–25), and elevation class 1821–1954 m are all factors that contribute to the wide distribution of the very high hazard (VHH) zone and high hazard (HH) zone in the southwestern area. Most likely, landslides occur on slopes with an angle of 14–25, according to previous landslide inventory data, with 82% of landslides occurring only on this slope class. The majority of landslide areas are covered with alluvial and colluvial soil. Furthermore, nearly 68% of past landslides were distributed following the elevation class of 1821–1954 m. This indicates that this elevation class is the most vulnerable to slope failure.

LHZ map validation

The landslide hazard map was validated with the help of past landslide locations. This was computed by overlaying landslide location data and the landslide hazard map prepared. According to the overlay analysis (Fig. 4B), 70% of past landslides were found in the very high hazard zone and 24% were in the high hazard zone. Therefore, 94% of past landslide locations were satisfactorily matched with the LHZ map. The remaining 3% of landslides are found in the moderate hazard zones, 2% are found in the low hazard zones, and 1% are found in the no hazard zones. Furthermore, the produced landslide hazard map was physically validated in the field in several regions, most notably in the very high hazard and high hazard zones. Landslide activities were observed in areas that defied very high hazard and high hazard zones.

Thus, it is reasonable to assume this landslide hazard map (LHZ) adequately demarcated the spatial and potential landslide hazard zones of the research area.

The present study area, including Aneded and Baso Liben districts, are frequently affected by landslides, which cause damage to infrastructure and property. For this study, eight conditioning factors, including lithology and soil mass, slope, elevation, aspect, curvature, land use land cover, distance from lineaments/fault, and distance from drainage, were considered. The landslide inventory map was created using a digital elevation model (DEM), Google Earth image, and extensive field investigation. The statistical relationship between conditioning factors and landslides was investigated using the inventory map, as was their probable contribution to landslides in the area. In this research, the conditioning factors were rated using a GIS-based statistical and probability method, and the landslide hazard map was generated using a customized raster calculation. In this study, landslide hazard evaluation showed that 17.15% (40.60 km2), 25.53% (60.45 km2), 28.04% (66.39 km2), 18.93% (44.83 km2), and 10.36% (24.54 km2) of area fall into the no hazard, low, moderate, high, and very high hazard classes, respectively.

The findings and results of the present study can provide principal and necessary information about the causes and main conditioning factors of landslide occurrences. The created LHZ map can be used as a baseline by researchers, local governments, planners, and other responsible agencies for decision making and land use planning in the surrounding area. Besides, frequently occurring landslides have damaged the farmland and houses and killed animals in the study area. Due to all these factors, some zones are potentially dangerous for any future habitation and development activities. Thus, there is an immediate need to implement mitigation measures in the very high hazard and high hazard zones, or such zones need to be avoided for habitation or any future developmental activities.

Declaration of Competing Interest

The authors declare that they have no known competing financial interests or personal relationships that could have appeared to influence the work reported in this paper.

Acknowledgments

The author would like to thank the reviewers for their valuable suggestions and comments. And also, thanks to the local respondents and the community residing in the area for providing important information and support in the field data collection process.

References

[1] R. Kumar, R. Anbalagan, Landslide susceptibility zonation in part of Tehri reservoir region using frequency ratio, fuzzy logic and GIS, J. Earth Syst. Sci. 124 (2) (2015) 431–448 https://doi.org/, doi:10.1007/s12040-015-0536-2.
[2] Q. Wang, W. Li, W. Chen, H. Bai, GIS-based assessment of landslide susceptibility using certainty factor and index of entropy models for the Qianyang county of Baoji city, China, J. Earth Syst. Sci. 124 (7) (2015) 1399–1415 https://doi.org/, doi:10.1007/s12040-015-0624-3.
[3] B. Ermias, T.K. Raghuvanshi, B. Abebe, Landslide Hazard Zonation (LHZ) around Alemketema Town, North Showa Zone, Central Ethiopia - GIS Based Expert Eval. Approach 10 (01) (2017) 33–44 https://doi.org/, doi:10.21276/ijee.2017.10.0106.
[4] D. Asmare, T. Hailemariam, Assessment of rock slope stability using slope stability probability classification (SSPC) system, around AlemKetema, Sci. Afr. 12 (2021) e00730 https://doi.org/, doi:10.1016/j.sciaf.2021.e00730.
[5] K. Woldearegay, Review of the occurrences and influencing factors of landslides in the highlands of Ethiopia: with implications for infrastructural development, Momona Ethiop. J. Sci. 5 (1) (2013) 3 https://doi.org/, doi:10.4314/mejs.v5i1.85329.
[6] W. Chen, X. Xie, J. Peng, J. Wang, Z. Duan, H. Hong, GIS-based landslide susceptibility modelling: a comparative assessment of kernel logistic regression, Naïve-Bayes tree, and alternating decision tree models, Geom., Nat. Hazards, Risk 8 (2) (2017) 950–973 https://doi.org/, doi:10.1080/19475705.2017.1289250.
[7] Mersha, T., & Meten, M. (2020). GIS-based landslide susceptibility mapping and assessment using bivariate statistical methods in Simada area, northwestern.
[8] F. Mengistu, K.V. Suryabhagavan, T.K. Raghuvanshi, E. Lewi, Landslide hazard zonation and slope instability assessment using optical and insar data: a case study from gidole town and its surrounding areas, Southern Ethiopia, Rem. Sens. Land 3 (1) (2019) 1–14 https://doi.org/, doi:10.21523/gcj1.19030101.
[9] Identification, A. (2003). Landslide hazard assessment and risk evaluation: limits and prospectives, (October 2002).
[10] I.A.K. Jadoon, M. Hinderer, A.B. Kausar, A.A. Qureshi, M.S. Baig, M. Basharat, W. Frisch, Structural interpretation and geo-hazard assessment of a locking line: 2005 Kashmir earthquake, western Himalayas, Environ. Earth Sci. 73 (11) (2015) 7587–7602 https://doi.org/, doi:10.1007/s12665-014-3929-7.
[11] C. Tesfa, K. Woldearegay, Characteristics and susceptibility zonation of landslides in Wabe Shebelle Gorge, southeastern Ethiopia, J. Earth Syst. Sci. 182 (2021) 104275 Mayhttps://doi.org/, doi:10.1016/j.jafrearsci.2021.104275.
[12] Chimidi, G., Raghuvanshi, T.K., & Suryabhagavan, K.V. (2017). Landslide hazard evaluation and zonation in and around Gimbi town, western Ethiopia — a GIS-based statistical approach. https://doi.org/ 10.1007/s12518-017-0195-x
[13] T. Hamza, T.K. Raghuvanshi, GIS based landslide hazard evaluation and zonation – a case from Jeldu District, Central Ethiopia, J. King Saud Univ. –Sci. 29 (2017) 151–165 https://doi.org/, doi:10.1016/j.jksus.2016.05.002.
[14] T.K. Raghuvanshi, J. Ibrahim, D. Ayalew, Slope stability susceptibility evaluation parameter (SSEP) rating scheme - an approach for landslide hazard zonation, J. Afr. Earth Sci. 99 (PA2) (2014) 595–612 https://doi.org/, doi:10.1016/j.jafrearsci.2014.05.004.
[15] X.Z. Li, Q. Xu, Application of the SSPC method in the stability assessment of highway rock slopes in the Yunnan province of China, Bull. Eng. Geol. Environ. 75 (2) (2016) 551–562 https://doi.org/, doi:10.1007/s10064-015-0792-z.
[16] A.K. Saha, R.P. Gupta, M.K. Arora, GIS-based landslide hazard zonation in the Bhagirathi (Ganga) Valley, Himalayas, Int. J. Rem. Sens. 23 (2) (2002) 357–369 https://doi.org/, doi:10.1080/01431160010014260.
[17] H. He, D. Hu, Q. Sun, L. Zhu, Y. Liu, A landslide susceptibility assessment method based on GIS technology and an AHP-weighted information content method: a case study of southern Anhui, China, ISPRS Int. J. Geoinf. 8 (6) (2019) https://doi.org/, doi:10.3390/ijgi8060266.
[18] D. Asmare, C. Tesfa, Application and Validation of the evaluation using slope stability susceptibility evaluation parameter rating system to debre werk area (Northwest Ethiopia), Geotech. Geol. Eng. 9 (2022) https://doi.org/, doi:10.1007/s10706-021-02039-9.
[19] J.S. Rawat, R.C. Joshi, Remote-sensing and GIS-based landslide-susceptibility zonation using the landslide index method in Igo River Basin, Eastern Himalaya, India, Int. J. Rem. Sens. 33 (12) (2012) 3751–3767 https://doi.org/, doi:10.1080/01431161.2011.633121.
[20] S. Das, R.K. Ray, G. Nain, GIS based landslide hazard zonation of Guwahati Region, Int. J. Eng. Dev. Res. 2 (4) (2014) 4005–4014 Dec 2014.
[21] Anbalagan, R., Kumar, R., Lakshmanan, K., Parida, S., & Neethu, S. (2015). Landslide Hazard Zonation Mapping Using Frequency Ratio and Fuzzy Logic approach, a Case Study of Lachung Valley, Sikkim. https://doi.org/ 10.1186/s40677-014-0009-y
[22] A. Abay, G. Barbieri, K. Woldearegay, GIS-based landslide susceptibility evaluation using analytical hierarchy process (AHP) approach: the case of Tarmaber District, Ethiopia, Momona Ethiop. J. Sci. 11 (1) (2019) 14 https://doi.org/, doi:10.4314/mejs.v11i1.2.
[23] T.K. Raghuvanshi, L. Negassa, P.M. Kala, GIS based Grid overlay method versus modeling approach - a comparative study for landslide hazard zonation (LHZ) in Meta Robi District of West Showa Zone in Ethiopia, Egypt. J. Rem. Sens. Space Sci. 18 (2) (2015) 235–250 https://doi.org/, doi:10.1016/j.ejrs.2015.08.001.
[24] El F. Bchari, B. Theilen-Willige, H. Ait Malek, Landslide hazard zonation assessment using GIS analysis at the coastal area of Safi (Morocco), in: Proceedings of the ICA, 2019, pp. 1–7, doi:10.5194/ica-proc-2-24-2019. 2(July)https://doi.org/.
[25] Y. Yi, Z. Zhang, W. Zhang, Q. Xu, C. Deng, Q. Li, GIS-based earthquake-triggered-landslide susceptibility mapping with an integrated weighted index model in Jiuzhaigou region of Sichuan Province, China, Nat. Hazards Earth Syst. Sci. 19 (9) (2019) 1973–1988 https://doi.org/, doi:10.5194/nhess-19-1973-2019.
[26] A. Clerici, S. Perego, C. Tellini, P. Vescovi, A GIS-based automated procedure for landslide susceptibility mapping by the Conditional Analysis method: the Baganza valley case study (Italian Northern Apennines), Environ. Geol. 50 (7) (2006) 941–961 https://doi.org/, doi:10.1007/s00254-006-0264-7.
[27] L. Ayalew, H. Yamagishi, The application of GIS-based logistic regression for landslide susceptibility mapping in the Kakuda-Yahiko Mountains, Central Japan, Geomorphology 65 (1–2) (2005) 15–31 https://doi.org/, doi:10.1016/j.geomorph.2004.06.010.
[28] C. Kıncal, Z. Li, J. Drummond, P. Liu, T. Hoey, J.-.P. Muller, Landslide susceptibility mapping using GIS-based vector grid file (VGF) validating with InSAR techniques: three Gorges, Yangtze River (China), AIMS Geosci. 3 (1) (2017) 116–141 https://doi.org/, doi:10.3934/geosci.2017.1.116.
[29] A. Ozdemir, A comparative study of the frequency ratio, analytical hierarchy process, artificial neural networks and fuzzy logic methods for landslide susceptibility mapping : Tas¸ Kent (Konya), Turkey, Geotech. Geol. Eng. 8 (2020) https://doi.org/, doi:10.1007/s10706-020-01284-8.
[30] R.K. Dahal, S. Hasegawa, N.P. Bhandary, P.P. Poudel, A. Nonomura, R. Yatabe, A replication of landslide hazard mapping at catchment scale, Geom., Nat. Hazards, Risk 3 (2) (2012) 161–192 https://doi.org/, doi:10.1080/19475705.2011.629007.
[31] Solaimani, K., & Mousavi, S.Z. (2013). Landslide susceptibility mapping based on frequency ratio and logistic regression models, 2557–2569. https://doi.org/ 10.1007/s12517-012-0526-5

[32] M. Sharma, R Kumar, GIS-based landslide hazard zonation: a case study from the Parwanoo area, Lesser and Outer Himalaya, H.P., India, Bull. Eng. Geol. Environ. 67 (1) (2008) 129–137 https://doi.org/, doi:10.1007/s10064-007-0113-2.
[33] I. Armaş, Weights of evidence method for landslide susceptibility mapping. Prahova Subcarpathians, Romania, Nat. Hazards 60 (3) (2012) 937–950 https://doi.org/, doi:10.1007/s11069-011-9879-4.
[34] H. Chang, N.K. Kim, The evaluation and the sensitivity analysis of GIS-based landslide susceptibility models, Geosci. J. 8 (4) (2004) 415–423 https://doi.org/, doi:10.1007/BF02910477.
[35] S.B. BAI, J. WANG, G.N. LÜ, P.G. ZHOU, S.S. HOU, S.N XU, GIS-based and data-driven bivariate landslide-susceptibility mapping in the three Gorges Area, China Project supported by the National Natural Science Foundation of China, Pedosphere 19 (1) (2009) 14–20 https://doi.org/, doi:10.1016/S1002-0160(08)60079-X.
[36] M. Conforti, G. Robustelli, F. Muto, S. Critelli, Application and validation of bivariate GIS-based landslide susceptibility assessment for the Vitravo river catchment (Calabria, south Italy), Nat. Hazards 61 (1) (2012) 127–141 https://doi.org/, doi:10.1007/s11069-011-9781-0.
[37] Z. Anis, G. Wissem, V. Vali, H. Smida, G. Mohamed Essghaier, GIS-based landslide susceptibility mapping using bivariate statistical methods in North-western Tunisia, Open Geosci. 11 (1) (2019) 708–726 https://doi.org/, doi:10.1515/geo-2019-0056.
[38] S. Mandal, K. Mandal, Bivariate statistical index for landslide susceptibility mapping in the Rorachu river basin of eastern Sikkim Himalaya, India, Spatial Inf. Res. 26 (1) (2018) 59–75 https://doi.org/, doi:10.1007/s41324-017-0156-9.
[39] A. Nandi, A. Shakoor, A GIS-based landslide susceptibility evaluation using bivariate and multivariate statistical analyses, Eng. Geol. 110 (1–2) (2010) 11–20 https://doi.org/, doi:10.1016/j.enggeo.2009.10.001.
[40] S.I. Elmahdy, M.M. Marghany, M.M. Mohamed, Application of a weighted spatial probability model in GIS to analyse landslides in Penang Island, Malaysia, Geomat., Nat. Hazards, Risk 7 (1) (2016) 345–359 https://doi.org/, doi:10.1080/19475705.2014.904825.
[41] D. Pathak, Geohazard assessment along the road alignment using remote sensing and GIS: case study of Taplejung-Olangchunggola-Nangma road section, Taplejung district, east Nepal, J. Nepal Geol. Soc. 47 (1) (2014) 47–56 https://doi.org/, doi:10.3126/jngs.v47i1.23103.
[42] L. Li, H. Lan, C. Guo, Y. Zhang, Q. Li, Y. Wu, A modified frequency ratio method for landslide susceptibility assessment, Landslides 14 (2) (2017) 727–741 https://doi.org/, doi:10.1007/s10346-016-0771-x.
[43] H. Khan, M. Shafique, M.A. Khan, M.A. Bacha, S.U. Shah, Landslide susceptibility assessment using frequency ratio, a case study of northern Pakistan, Egypt. J. Rem. Sens. Space Sci. (2018) XXXXhttps://doi.org/, doi:10.1016/j.ejrs.2018.03.004.
[44] B. Neuhäuser, B. Terhorst, Landslide susceptibility assessment using "weights-of-evidence" applied to a study area at the Jurassic escarpment (SW-Germany), Geomorphology 86 (1–2) (2007) 12–24 https://doi.org/, doi:10.1016/j.geomorph.2006.08.002.
[45] B. Pradhan, H.J. Oh, M. Buchroithner, Weights-of-evidence model applied to landslide susceptibility mapping in a tropical hilly area, Geomat., Nat. Hazards, Risk 1 (3) (2010) 199–223 https://doi.org/, doi:10.1080/19475705.2010.498151.
[46] S. Lee, Application of logistic regression model and its validation for landslide susceptibility mapping using GIS and remote sensing data, Int. J. Rem. Sens. 26 (7) (2005) 1477–1491 https://doi.org/, doi:10.1080/01431160412331331012.
[47] J. Choi, H.J. Oh, H.J. Lee, C. Lee, S. Lee, Combining landslide susceptibility maps obtained from frequency ratio, logistic regression, and artificial neural network models using ASTER images and GIS, Eng. Geol. 124 (1) (2012) 12–23 https://doi.org/, doi:10.1016/j.enggeo.2011.09.011.
[48] H. Hemasinghe, R.S.S. Rangali, N.L. Deshapriya, L. Samarakoon, Landslide susceptibility mapping using logistic regression model (a case study in Badulla District, Sri Lanka), Procedia Eng. 212 (2018) 1046–1053 https://doi.org/, doi:10.1016/j.proeng.2018.01.135.
[49] F. Mancini, C. Ceppi, G. Ritrovato, GIS and statistical analysis for landslide susceptibility mapping in the Daunia area, Italy, Nat. Hazards Earth Syst. Sci. 10 (9) (2010) 1851–1864 https://doi.org/, doi:10.5194/nhess-10-1851-2010.
[50] S. Mashari, K. Solaimani, E. Omidvar, Landslide susceptibility mapping using multiple regression and GIS tools in Tajan Basin, North of Iran, Environ. Nat. Resour. Res. 2 (3) (2012) 43–51 https://doi.org/, doi:10.5539/enrr.v2n3p43.
[51] R. Sankar Jakka, B. Mouli Marrapu, Landslide hazard zonation methods: a critical review, Int. J. Civil Eng. Res. 5 (3) (2014) 215–220.
[52] V. Vakhshoori, M. Zare, Landslide susceptibility mapping by comparing weight of evidence, fuzzy logic, and frequency ratio methods, Geomat., Nat. Hazards, Risk 7 (5) (2016) 1731–1752 https://doi.org/, doi:10.1080/19475705.2016.1144655.
[53] G. Leonardi, R. Palamara, F. Cirianni, Landslide susceptibility mapping using a fuzzy approach, Procedia Eng. 161 (2016) 380–387 https://doi.org/, doi:10.1016/j.proeng.2016.08.578.
[54] P. Kayastha, S.M. Bijukchhen, M.R. Dhital, F. De Smedt, GIS based landslide susceptibility mapping using a fuzzy logic approach: a case study from Ghurmi-Dhad Khola area, Eastern Nepal, J. Geol. Soc. India 82 (3) (2013) 249–261 https://doi.org/, doi:10.1007/s12594-013-0147-y.
[55] P.K.C. Ray, S. Dimri, R.C. Lakhera, S. Sati, Fuzzy-based method for landslide hazard assessment in active seismic zone of Himalaya, Landslides 4 (2) (2007) 101–111 https://doi.org/, doi:10.1007/s10346-006-0068-6.
[56] A.M. Gbadebo, O.H. Adedeji, A.S. Edogbo, GIS-based landslide susceptibility assessment in Eyinoke Hilly Area of Okeigbo, SW, Nigeria, J. Appl. Sci. Environ. Manag. 22 (6) (2018) 917 https://doi.org/, doi:10.4314/jasem.v22i6.13.
[57] R. Schicker, V. Moon, Geomorphology Comparison of bivariate and multivariate statistical approaches in landslide susceptibility mapping at a regional scale, Geomorphology (2012) 40–57 *161–162*https://doi.org/, doi:10.1016/j.geomorph.2012.03.036.
[58] A. Yalcin, GIS-based landslide susceptibility mapping using analytical hierarchy process and bivariate statistics in Ardesen (Turkey): comparisons of results and confirmations, Catena 72 (1) (2008) 1–12 https://doi.org/, doi:10.1016/j.catena.2007.01.003.
[59] J.B. Nsengiyumva, R. Valentino, Predicting landslide susceptibility and risks using GIS-based machine learning simulations, case of upper Nyabarongo catchment, Geomat., Nat. Hazards, Risk 11 (1) (2020) 1250–1277 https://doi.org/, doi:10.1080/19475705.2020.1785555.
[60] J.B. Nsengiyumva, G. Luo, L. Nahayo, X. Huang, P. Cai, Landslide susceptibility assessment using spatial multi-criteria evaluation model in Rwanda, Int. J. Environ. Res. Public Health 15 (2) (2018) https://doi.org/, doi:10.3390/ijerph15020243.
[61] J. Varo, T. Sekac, S.K. Jana, Landslide hazard zonation from a GIS perspective and urban planning solutions in Central –division of Fiji Islands, Int. J. Innov. Technol. Explor. Eng. 8 (12S) (2019) 352–361 https://doi.org/, doi:10.35940/ijitee.l1091.10812s19.
[62] Kailas, A., Shajan, G., Joy, S., & George, G.K. (2018). Landslide hazard zonation (LHZ) mapping of Attappady, Kerala using GIS, 3808–3812.
[63] E.S. Jishnu, A.J. K, S. Sreedhar, G Basil, Hazard mapping of landslide vulnerable zones in a rainfed region of southern peninsular india- a geospatial perspective, Int. Res. J. Eng. Technol. (IRJET) 4 (7) (2017) 1350–1357 Retrieved from https://irjet.net/archives/V4/i7/IRJET-V4I7293.pdf .
[64] S. Dragićević, T. Lai, S. Balram, GIS-based multicriteria evaluation with multiscale analysis to characterize urban landslide susceptibility in data-scarce environments, Habitat Int. 45 (P2) (2014) 114–125 https://doi.org/, doi:10.1016/j.habitatint.2014.06.031.
[65] L. Dahoua, V.Y. Savenko, R. Hadji, GIS-based technic for roadside-slope stability assessment: an bivariate approach for A1 East-West Highway, North Algeria, Min. Sci. 24 (2017) 117–127 https://doi.org/, doi:10.5277/msc172407.
[66] Sensing, R., Analysis, B., Gashaw, T., Bantider, A., & Mahari, A. (2014). Evaluations of land use /land cover changes and land degradation in Dera full length research paper evaluations of land use / land cover changes and land degradation in Dera District, Ethiopia : GIS and remote sensing based analysis, (June). https://doi.org/ 10.12983/ijsres-2014-p0199-0208
[67] R. Raman, M. Punia, The application of GIS-based bivariate statistical methods for landslide hazards assessment in the upper Tons river valley, Western Himalaya, India, Georisk 6 (3) (2012) 145–161 https://doi.org/, doi:10.1080/17499518.2011.637504.
[68] N. Nepal, J. Chen, H. Chen, X. Wang, T.P. Pangali Sharma, Assessment of landslide susceptibility along the Araniko Highway in Poiqu/Bhote Koshi/Sun Koshi Watershed, Nepal Himalaya, Prog. Disas. Sci. 3 (2019) 100037 https://doi.org/, doi:10.1016/j.pdisas.2019.100037.
[69] B. Prashad Bhatt, K. Datt Awasthi, B. Prasad Heyojoo, T. Silwal, G Kafle, Using geographic information system and analytical hierarchy process in landslide hazard zonation, Appl. Ecol. Environ. Sci. 1 (2) (2013) 14–22 https://doi.org/, doi:10.12691/aees-1-2-1.
[70] M. Foumelis, E. Lekkas, I. Parcharidis, Landslide susceptibility mapping by GIS-based qualitative weighting procedure in Corinth area, Bull. Geol. Soc. Greece 36 (2) (2018) 904 https://doi.org/, doi:10.12681/bgsg.16840.

[71] E. Nohani, M. Moharrami, S. Sharafi, K. Khosravi, B. Pradhan, B.T. Pham, A. Melesse, Landslide susceptibility mapping using different, Water (Basel) 11 (7) (2019) 1402.
[72] E.A. Michael, S. Samanta, Landslide vulnerability mapping (LVM) using weighted linear combination (WLC) model through remote sensing and GIS techniques, Model. Earth Syst. Environ. 2 (2) (2016) 1–15 https://doi.org/, doi:10.1007/s40808-016-0141-7.
[73] F.C. Dai, C.F. Lee, Terrain-based mapping of landslide susceptibility using a geographical information system: a case study, Can. Geotech. J. 38 (5) (2001) 911–923 https://doi.org/, doi:10.1139/t01-021.
[74] M.L. Süzen, V. Doyuran, Data driven bivariate landslide susceptibility assessment using geographical information systems: a method and application to Asarsuyu catchment, Turkey, Eng. Geol. 71 (3–4) (2004) 303–321 https://doi.org/, doi:10.1016/S0013-7952(03)00143-1.
[75] B.F.D. Wahono, ITC MSc Thesis, ITC MSc Thesis, 106, 2010.
[76] T. Hamza, T.K. Raghuvanshi, GIS based landslide hazard evaluation and zonation – a case from Jeldu District, Central Ethiopia, J. King Saud Univ. - Sci. 29 (2) (2016) 151–165 https://doi.org/, doi:10.1016/j.jksus.2016.05.002.
[77] Vishwakarma, C.A., Asthana, H., Singh, D., Pant, M., & Sen, R. (2017). GIS Based Bi-Variate Statistical Approach for Landslide Susceptibility Mapping of South District, Sikkim, 13661–13674. https://doi.org/ 10.15680/IJIRSET.2017.0607123
[78] I. Milevski, S. Dragićević, M. Zorn, Statistical and expert-based landslide susceptibility modeling on a national scale applied to North Macedonia, Open Geosci. 11 (1) (2019) 750–764 https://doi.org/, doi:10.1515/geo-2019-0059.
[79] R. Kumar, R. Anbalagan, Landslide susceptibility mapping of the Tehri reservoir rim area using the weights of evidence method, J. Earth Syst. Sci. (6) (2019) 128 https://doi.org/, doi:10.1007/s12040-019-1159-9.